의학석사 학위논문

Cysteine-rich angiogenic protein 61-induced ectopic mineralization is mediated by activation of matrix metalloproteinases in vascular smooth muscle cells

혈관 평활근 세포의 CYR61 단백에 의해 매개되는 이소성 무기화 작용은 기질금속단백분해효소의 활성화에 의해 매개된다

2016년 1월

서울대학교 대학원

분자의학 및 바이오제약학과

분자의학 및 바이오제약학 전공

김 치 훈

Cysteine-rich angiogenic protein 61-induced ectopic mineralization is mediated by activation of matrix metalloproteinases in vascular smooth muscle cells

지도교수 김 효 수

이 논문을 의학석사 학위논문으로 제출함

2016년 1월

서울대학교 대학원

분자의학 및 바이오제약학과

분자의학 및 바이오제약학 전공

김 치 훈

김치훈의 석사 학위논문을 인준함

2016년 1월

위 원 장 이 동 수 (인)

부위원장 김 효 수 (인)

위 원 박 경 수 (인)

Abstract

Background: Cysteine-rich angiogenic protein 61 (CYR61) was reported to be induced by angiotensin II in vascular smooth muscle cells (VSMCs), and it is a key regulatory molecule in ectopic mineralization of osteogenic transdifferentiated VSMCs. But, exact molecular mechanism of CYR61-induced mineralization is unclear, so we explored downstream effector molecule of CYR61.

Methods and Results: VSMCs harvested from thoracic aortas of male C57BL6 mice were transfected with adenoviral vector containing Cyr61 (Ad-CYR61), and then microarray analysis was performed to evaluate the effects of CYR61 on VSMC mineralization. Several matrix metalloproteinases such as MMP-13, MMP-3 and MMP-10 were immediately increased by 7.9, 6.5, and 2.0-folds after 24 hours of transfection. However, tissue inhibitors of metalloproteinases such as TIMP-3 and TIMP-2 were reduced by 52% and 71%, respectively (all $p<0.05$). Real-time PCR confirmed MMP-13 gene induction by 33±13 folds compared to control adenovirus-transfected VSMCs ($p<0.05$). Although mRNA expression of MMP-9 was not found to be increased, gelatin zymography showed an augmented enzymatic activity of MMP-9 by Ad-CYR61 transfection, which was significantly decreased by siRNA for MMP-13. In the light microscopic analysis with Von Kossa staining or electron microscopic

examinations, dominant negative adenoviral vector for c-Jun and broad spectrum MMP inhibitor doxycycline can minimize or attenuate CYR61-medated ECM disruption or ectopic mineralization.

Conclusion: These findings demonstrate that CYR61-mediated MMP activation is important to induce vascular calcification in the milieu of systemic inflammation. Therapies targeting to CYR61 or MMPs may modulate vascular calcification and could have clinical implications.

Key words: Cysteine-rich angiogenic protein 61, Matrix metalloproteinase, Mineralization, Vascular calcification

Student Identification Number: 2010-22901

Contents

List of Tables

List of Figures

List of Abbreviations

BMP2	bone morphogenic protein 2
Ad-AS-Cyr61	adenoviral vector expressing antisense Cyr61 cDNA fragment
Ad-Cyr61	adenoviral vector containing Cyr61
Ad-DN-c-Jun	adenoviral vector containig dominant-negative mutant of c-Jun
Ad-GFP	adenoviral vector expressing green fluorescent protein
Ad-β-gal	adenoviral vector containing bacterial β-galactosidase gene
AP-1	activator protein-1
CCN1	CYR61, cysteine-rich angiogenic protein 61
CCN2	pro-fibrotic connective tissue growth factor
CYR61	cysteine-rich angiogenic protein 61
DMEM	Dulbecco's modified Eagle's medium
ECM	extracellular matrix
FBS	fetal bovine serum
GADPH	glyceraldehyde 3-phosphate dehydrogenase
JNK	c-Jun N-terminal kinase
MMP	matrix matalloproteinases
MOI	multiplicity of infection
ROS	reactive oxygen species
Runx2	Runt-related transcription factor 2
SEM	scanning electron microscopy
siRNA	small interfering ribonucleic acid
TEM	transmission electron microscopy
VSMC	vascular smooth muscle cells

Introduction

Vascular calcification refers to ectopic deposition and crystallization of hydroxyapatite in the atheroma of the arterial intima or medial layer of the vessel wall. Calcium phosphate crystal deposition in the vasculature is not a result of simple and passive degeneration. Instead, in addition to the loss of local or systemic calcium phosphate homeostasis, ectopic calcification is caused by diverse initiating and amplifying molecular mechanisms. As an instance, characteristic phenotypical changes in vascular smooth muscle cells (VSMCs) may be eventually connected to nanocrystal deposition in the damaged elastic fibers (1-3). Indeed, vascular smooth muscle cells play a critical role in the pathogenesis of calcification. Ever since osteoblast-related bone morphogenetic protein 2 (BMP2) was found in calcified human atherosclerotic lesions (4), many researchers have noted that some VSMCs with phenotypic plasticity could be transdifferentiated into cells with osteochondrogenic characteristics. In the calcifying arterial wall, bone-related genes such as Runx2/Cbfa1, Msx2, alkaline phosphatase and osteopontin could be consequently expressed in these transdifferentiated VSMCs (5, 6). Under the circumstances of imbalanced inorganic phosphate homeostasis, this phenotypic transition of VSMCs may be subsequently linked to the alteration of crystal formation and growth dynamics (3). In this context, matrix vesicles which contain calcium phosphate crystals seem to be released by VSMCs in calcifying

atheroma or arterial medial layer as nucleating agents (7, 8). And, apoptotic bodies from VSMCs can act as the other key nucleating factor for crystal deposition in the calcifying aortic wall (9).

These processes are known to be initiated by inflammation. Local inflammation precede osteogenic conversion of VSMCs (10). However, exact molecular cascade still remains elusive to date. For example, although some studies have sporadically pointed that angiotensin Ⅱ may be one of key regulatory molecules, little is known about detailed downstream signaling pathways. Aside from the indirect effect on aldosterone and mineralocorticoid receptors (11), angiotensin Ⅱ can stimulate osteoblastic transdifferentiation of VSMCs and extracellular matrix (ECM) mineralization via type I angiotensin receptor. (12) And as addressed in the previous report from our laboratory, this change was mediated by cysteine-rich angiogenic protein 61 (CYR61) activation (13). Osteogenic transdifferentiation of VSMCs and mineralization were significantly reduced by transfection of antisense-CYR61 adenovirus in our previous report.

This finding suggests that metabolic and inflammatory stimuli can directly provoke vascular calcification, and again, this change may be interrelated to complex signaling pathways of matrix remodeling. In fact, CYR61 is a member of matricellular protein CCN family and have important roles in wound healing and matrix remodeling (14). Because various matrix matalloproteinases (MMPs) as well as growth hormones and cytokines can be regulated by CCN proteins,

angiotensin Ⅱ-regulated CYR61 activation may be connected to disruption of the ECM. Since exact downstream effectors of angiotensin Ⅱ and CYR61 are not yet certain in the altered VSMCs, this hypothesis may provide interesting clues to molecular mechanisms of vascular calcification. CYR61 activation in VSMCs might induce MMP-mediated ECM disruption, and then this change might be closely connected to ectopic calcium phosphate crystal deposition in the vasculature. Thus, we explored molecular mechanisms beyond CYR61, and tested the role of CYR61-MMP axis using cultured mouse VSMCs.

Materials and methods

Preparation and cell culture for VSMCs

Cultured VSMCs were obtained from the aorta tissue of male sex C57BL/6J mice (KBT Oriental Co Ltd., Charles River Grade, Tosu, Saga, Japan). We used 6-week-old mice for isolation of VSMCs and subsequent experiments. 6 to 7-passage VSMCs were cultured and incubated at 5% CO_2 chamber under the temperature of 37°C in Dulbecco's modified Eagle's medium (DMEM) solution (GIBCOBRLCo.) with 10% fetal bovine serum (FBS,Cambrex) and 1% antibiotic/antimycotic solution (GIBCOBRLCo.). Induction media for calcification were used to enhance calcifying potency, and this was supplemented with DMEM and 15% FBS, 1% antibiotics, 6mmol/L calciumchloride ($CaCl_2$), 10mmol/L sodium pyruvate, 50g/mL ascorbic acid, and 10mmol/L glycerophosphate. All animal experiments in this study were reviewed by a regulatory committee of Seoul National University Hospital Biomedical Research Institute (IACUC, Institutional Animal Careand Use Committees) for the care and use of animals, the animal studies were performed after receiving approval of IACUC (IACUC approval No. 10-0231).

Gene transfer using adenoviral vectors expressing and suppressing CYR61

To evaluate CYR61-mediated mineralization mechanisms, we used

mouse Cyr61-expressing adenovirus vector (Ad-Cyr61) as previously described (15). In brief, using total RNA from VSMCs of C57BL6 mice, full-length rat Cyr61 cDNA was generated by RT-PCR with the following primer: 5'-aggagatctatgagctccagcaccatcaag-3' and 5'-gctaagcttctttagtccctgaacttgtgg-3'. cDNA of Cyr61 was cloned into pMD19-T simple vector and then additionally subcloned into pAdTrackCMV to get pAdTrack-Cyr61. To generate Ad-Cyr61, the shuttle vector was used according to the manufacturer's recommendations. An adenoviral vector expressing green fluorescent protein (GFP; Ad-GFP) was used as a control. Recombinant adenoviral vector expressing antisense Cyr61 cDNA fragment (Ad-AS-Cyr61) was also used as an another control to interfere with Cyr61 protein expression in cultured cells (16). After cloning a 386-nucleotide fragment overlapping the initial Cyr61 ATG translation start site and using CMV promoter, Ad-AS-Cyr61 was prepared with an adenoviral shuttle vector co-transfection. The antisense cDNA fragment was generated by PCR amplification using the following primer: 5'-ggcaggtacccgccacaatgagctccagcac-3' and 5'-ggcaagatcttgcactggtgtttacagttgggc-3'. All adenovirus was replication deficient and used with 50 multiplicity of infections (MOIs) for 24 hours at 37°C and 5% CO_2/95% air without apparent cytotoxicity. For transfection, DMEM media and 2% charcoal stripped serum were used at the day before, an d media was changed to DMEM and 10% charcoal stripped serum at the time of transfection. Transfection efficiencies of greater than 90% at post-transfection

24-hour were maintained during the entire transfection process. As each adenoviral vector contained GFP sequence, transfection efficacy was confirmed by visualization of the green fluorescence of transfected cells.

Calcification stimulation with angiotensin II

After transfection, angiotensin II (Sigma, A9525 with a concentration of 0.1μmol/L) was treated to stimulate calcification process. To perform this treatment, cultured VSMCs were prepared on a 6-well plate with the calcification media as aforementioned.

Microarray analysis

Affymatrix gene chip microarray analysis (Magic-II 10K oligonucleotide microarray, Macrogen) was done as previously described (17) to evaluate downstream effector molecules of CYR61-mediated VSMCs calcification. Using RNeasy mini spin columns (Qiagen), cultured and transfected VSMCs were harvested for total RNA preparation. Total RNA was converted to biotin-labeled cRNA and hybridized to U95A oligonucleotide arrays containing 12,532 sequences and then gene expression data were analyzed. After the treatment with angiotensin II, Ad-Cyr61-transfected VSMCs were harvested to evaluate full range of gene expression profile of CYR61-mediated calcification. And for comparison, Ad-AS-Cyr61 and

Ad-GFP-infected VSMCs with angiotensin Ⅱ treatment were also harvested to show upregulated gene expression profile. Ad-GFP-treated VSMCs without angiotensin Ⅱ were also harvested as a control group. Every RNA harvest was done at the time of 4 hours and 24 hours after the transfection, and gene expression profiles were analyzed separately. The transcriptome patterns of these experimental groups were compared in a duplicate and replicate design. With the duplicated control Ad-GFP and Ad-AS-Cyr61 treated VSMCs, insignificant genes were filtered out, and noticeable deviations in signal intensity were caught for further analysis. Absolute values of signal intensity over 100 units, and signal increment or decrement more than twofold were used as the criteria of significance. The same filtration process was performed in Ad-Cyr61 and Ad-GFP comparison experiment. The genes that passed the filtration in both replicated experiments were considered as genes significantly regulated by Cyr61. To exclude the nonspecific effect of viral infection, we also examined the transcription profiles between mock-infected VSMCs and Ad-GFP-transfected VSMCs in a duplicate and replicate manner. The same filtration process was applied, and Cyr61-mediated changes in expression levels of target genes were then identified.

Construction of Ad-DN-c-Jun

After we found that matrix metalloproteinase-13 (MMP-13,

collagenase-3) was activated in Ad-Cyr61 transfected VSMCs (see results), we constructed dominant-negative mutant of c-Jun, also called as TAM67, to evaluate the effect of MMPs on mineralization process. c-Jun protein is a major substrate c-Jun N-terminal kinases (JNKs), and phosphorylated c-Jun can constitute a AP-1 (activator protein-1) heterodimer complex with c-fos protein. In addition to MMP-13, most MMP promoters have an AP-1 binding site for their transcriptional regulation. In this way, c-Jun N-terminal kinases (JNKs) can regulate the expression of MMPs especially in VSMCs (18, 19).

With the aid of polymerase chain reaction, dominant-negative mutant of c-Jun (DN-c-Jun) was generated by removing the trans-activation domain of amino acids 3 to 122 of wild type c-Jun. DN-c-Jun has the DNA binding domain of wild type c-Jun (20). According to the method used in the previous report (20, 21), recombinant replication-defective E1 and E3 adenoviral vectors expressing the DN-c-Jun gene (Ad-DN-c-Jun) were constructed by using an adenovirus expression vector kit (Takara Biomedicals). cDNA encoding DN-c-Jun was inserted into a cosmid cassette vector, PaxCAwt, which possesses the CAG promoter and was composed of a cytomegalovirus enhancer, chicken β-actin promoter, and rabbit β-globin poly(A) signal. Using this cosmid vector, a recombinant adenoviral vector was constructed by in vitro homologous recombination. In addition, adenoviral vector containing bacterial β-galactosidase gene (Ad-β-gal) were also constructed as a

negative control of Ad-DN-c-Jun with the same ways of Ad-DN-c-Jun. Recombinant adenoviruses containing Cyr61 cDNA gene construct were also produced in the same manner to compare the level of expression of MMPs. The titer of the adenovirus was determined by limiting dilution and expressed as plaque-forming units.

Real-time RT-PCR and immunoblot analysis

VSMCs were scraped and lysed in the Trizol solution (Invitrogen Life Technology), and RNA was extracted by chloroform and isopropanol precipitation. And then to obtain the supernatant, extracted RNA solution was centrifuged and stored at -80°C. Complementary DNA for Cyr61, MMP-9 (gelatinase B), MMP-13, Runt-related transcription factor 2 (Runx2), glyceraldehyde 3-phosphate dehydrogenase (Gapdh) were synthesized after reverse transcription from extracted RNAs. RT-PCR was examined with the reverse transcription kit (SuperScript® VILO™ cDNA synthesis kit), and respective primer sequences, product sizes, annealing temperatures of each primer for RT-PCR summarized in Table 1. Using the comparative CT (threshold cycle, ddCT) method, relative RNA expressions were quantitated with DataAssist software (ThermoScientific).

Immunoblot (Western blot) assays were also performed by the method published in other previous report. (22) Briefly, 4 groups of

VSMCs were treated with of Ad-Cyr61, Ad-Cyr61 and Ad-DN-c-Jun, Ad-Cyr61 and 10μM/L of doxycycline (23) and control GFP adenoviral vector respectively. Transfection of viral vectors were performed with 50 MOIs of each vectors. And then, transfected VSMCs were treated with 10^{-7}mol/Langiotensin Ⅱ and these cells were incubated in calcification media upto 3, 5, 7 and 14 days after the transfection. 4 groups of VSMCs were harvested, protein extract (20μg per each sample) were separated on 10% SDS-PAGE gel and transferred onto polyvinylidene difluoride (PVDF) membrane (Bio-Rad Laboratories). The membranes were blocked with 5% skimmed milk in 10mM/L Tris buffer (adjusted to pH 8.0), 150mM/L sodium chloride, and 0.1% TBS-T buffer, incubated with primary antibodies for 1 hour, and washed with TBS-T buffer. These preparations were incubated with secondary antibodies conjugated to horseradish peroxidase (GE Healthcare Life Sciences Inc.) for 1 hour, washed again, and were identified with enhanced chemi-luminescence (New England Biolabs Inc.). For detection of mouse CYR61, MMP-13, RUNX2 and GAPDH, samples were probed with respective primary antibodies (all from Santa Cruz Biotechnology Inc.), and Amersham ECL-PLUS western blotting detection reagents (GE Healthcare Life Sciences Inc.) were used for probe detection.

Sample preparation for reversal experiment with JNK/MMP inhibition

To examine the role of MMP expression in transfected VSMCs, we designed a reversal experiment. VSMCs were transfected with Ad-β-gal and Ad-Cyr61, and then for JNK pathway inhibition, co-transfection with adenoviral vector expressing a dominant-negative mutant c-Jun (Ad-DN-c-Jun). Preparation methods and conditions for transfection were the same as mentioned above. Meanwhile, separate VSMCs colony which was transfected with Ad-Cyr61 treated with a broad-spectrum MMP inhibitor, 10μM/L of doxycycline just after the transfection. After the incubation period in DMEM media, these four comparators were harvested in day 1, 3, 5, 7 and 14. RT-PCR and immunoblotting were performed using the extracts from these comparators.

Gelatin zymography and blocking experiment for MMP-9

Gelatin zymography was performed using a previously described method. (22) In short, samples of media ($2x10^5$ cells seeded in each well) conditioned by different transfection and treatment scheme were separated on an 10% SDS-polyacrylamide gel containing 0.2% gelatin. After electrophoresis, gels were washed with 2.5% Triton X-100 solution and incubated at 37°C for 16 to 18 hours in buffer solution (0.15mM/L Tris (adjusted to pH 8.0), 2.5mM/L calcium chloride, and 0.02% sodium azide), rinsed again with 10% trichloroacetic acid. And then, this preparation was stained with 0.05% Coomassie Brilliant Blue R250 (SigmaCo.) and the location of gelatinolytic activity was

detected as clear bands. Enzymatic activity of MMP-9 (92kDa pro-MMP-9 and 83kDa active MMP-9) was examined with this method, Ad-Cyr61-transfected VSMCs were harvested for this purpose at day 0, 1, 3, 5, 7 and 14.

And enzymatic activity of MMP-9 in Ad-Cyr61 transfected VSMCs was compared with those of Ad-DN-c-Jun or doxycycline co-treated VSCMs at the time of post-transfection day 3. MMP-2 (72kDa, pro-MMP-2) was used as a control in this experiment. In addition to these experiments, we additionally performed blocking experiment using small interfering RNA (siRNA) oligonucleotides for MMP-13. Detailed description of siRNA transfection was previously reported. (24) To be short, siRNA for MMP-13 and GFP (SI02733815 and SI00288183 respectively, purchased from Qiagen) were used to treat VSMCs following the manufacturer's instructions. After the transfection with Ad-Cyr61 adenoviral vector or control Ad-β-gal vector, 250pmol of MMP-13 or GFP siRNA were treated to $8x10^5$ cells of each cell groups at the time of post-transfection day3. Treated cells were then harvested and enzymatic activities of MMP-9 were analyzed with gelatin zymography after the nucleofection and 24-hour incubation.

Scanning and transmission electron microscopy

Electron microscopic examination was performed to evaluate the effect of CYR61-mediated MMP expressions on cellular morphology.

Similar to other experiments, this examination was done with the same test and control groups. VSMCs were cultured from mice and then infected with adenoviral vectors of Ad-β-gal, Ad-Cyr61, Ad-Cyr61 plus Ad-DN-c-Jun. Separate cell cultures with Ad-Cyr61 transfection was again treated with doxycycline to suppress the effect of MMPs. These four groups of VSMCs were incubated in DMEM media and charcoal stripped serum for 3 days after the transfection, and examined using electron microscopy (JEOL Co.) at the Clinical Research Institute of Seoul National University Hospital.

For scanning electron microscopy (SEM), VSMCs were directly cultured on Falcon cell culture membrane. These samples were fixed using 1mL of 2% glutaraldehyde (Sigma-Aldrich) at 4°C for 2 hours. Then, these samples were washed with phosphate-buffered saline, dehydrated by soaking in increasing concentrations of ethanol (from 30% to 100%) and dried with hexamethyldisilazane solution. Gold-palladium alloy and aluminum stub were used to prepare the SEM examination.

For transmission electron microscopy (TEM), VSMCs were cultured and incubated with the same manner. After removal of the culture membrane, cohesive VSMCs pellets were made by brief spin. These pellets were fixed and dehydrated, and then embedded into the embedding media. Silver-to-gold thin sections were obtained and mounted on uncoated grids. TEM examination was performed after the double staining with aqueous saturated uranyl acetate and

Reynolds lead citrate.

Von Kossa staining for examining ectopic mineralization

To reveal mineralization potential of cultured VSMCs, we used von Kossa staining before the light microscopy examination. Staining method is the same to the previous description. (25) All VSMCs were incubated upto 14 days after the transfection. After the fixation of VSMCs in 0.1% glutaraldehyde with phosphate-buffered saline, cultured VSMC monolayer on the cover glass was rinsed with distilled water. VSMC monolayer was incubated with 1% silver nitrate solution in clear glass and was exposed to ultraviolet light for 20 minutes. Glass slides were again rinsed with distilled water several times, and unreacted silver was removed with 5% sodium thiosulfate for 5 minutes. After washing with distilled water again, slides were counterstained with nuclear fast red for 5 minutes, and microscopic examination was done.

Statistical analysis

All numerical data are presented as mean±standard deviation. Mann-Whitney U test was used to compare the results of small size sample data. In regard to statistical probability, cutoff value of 0.05 was considered as statistically significant.

Results

Genes related to dynamics of extracellular matrix proteins were altered after the transfection of Ad-Cyr61

Microarray analysis was performed to evaluate the effect of CYR61 on VSMC calcification. The result is summarized in Table 2. After the transfection with Ad-Cyr61 adenoviral vector, gene expression of several matrix metalloproteinases such as MMP-13, MMP-3, MMP-10, and MMP-8 were immediately increased. And these changes were sustained upto 24 hours after the transfection (by 7.9, 6.5, 2.0 and 2.0-fold at the time of 24 hours after the transfection). Although level of expression of these MMPs was slightly depressed as time passed, these expression profiles were distinctly different to those of tissue inhibitors of matrix metalloproteinases (TIMPs) or procollagen family genes. Gene transcription levels of TIMP-3 and TIMP-2 were reduced by 28% and 38% after 24 hours of Ad-Cyr61 transfection, respectively ($p<0.05$ for comparisons with MMPs). Various procollagen genes were also reduced with varying degrees. This microarray result suggests that dynamics of extracellular matrix (ECM) might be disrupted in the process of CYR61-mediated VSMCs mineralization.

The effect of CYR61 is mediated by JNK pathway

Transfection experiments using adenoviral vectors were successful,

and CYR61 protein expression was induced by 20.3 folds in VSMCs after 16 hours of transfection. Added to this, immunoblot analysis revealed that CYR61-induced MMP-13 expression was mediated by JNK pathway (Figure 1). Ad-Cyr61 adenoviral vector-transfected mouse VSMCs were incubated in calcification induction media with the treatment of angiotensin Ⅱ, and then protein expression of CYR61 and MMP-13 proteins was compared to that of VSMCs using Ad-Cyr61 and Ad-DN-c-Jun co-transfection. Compared to Ad-Cyr61-transfected VSMCs, Ad-DN-c-Jun co-transfection did not result in noticeable decrements of CYR61 protein expression. But instead, MMP-13 expression was markedly decreased by Ad-DN-c-Jun co-transfection even from the time of day 3, and this effect was sustained upto day 14. Because control GFP vector-treated VSMCs were also incubated in calcification media and angiotensin Ⅱ, CYR61 and MMP-13 expression in these VSMCs were comparable to Ad-Cyr61-treated VSMCs after the time of day 7. But, suppressed MMP-13 expression in Ad-Cyr61 and Ad-DN-c-Jun co-treated VSMCs was prominent even after this period of time. Osteogenic potential of transfected VSMCs were confirmed with primary antibody for RUNX2, we also checked again that CYR61 was important inducing factor for osteogenic transdifferentiation as well as MMP-13 expression in mouse VSMCs. At day 3, in contrast to Ad-Cyr61 treated VSMCs, RUNX2 as well as MMP-13 was not identifiable in control GFP vector-treated VSMCs. But as time passed by, CYR61 and RUNX2 expression became clear also in these VSMCs.

Meanwhile, RUNX2 expression was not hampered by Ad-DN-c-Jun or doxycycline administration. Doxycycline treatment for Ad-Cyr61-transfected VSMCs also did not significantly reduce protein expressions of CYR61 in this immunoblot analysis.

CYR61 induced MMP-13, but not MMP-9, shortly after the transfection

Quantitative RT-PCR at the time of 3 days after the Ad-Cyr61 transfection showed that, at least shortly after the transfection, gene expression of MMP-13, but not MMP-9 was markedly provoked by CYR61 (Figure 2). MMP-13 expression of Cyr61-transfected VSMCs was clearly higher than that of control group which was transfected with Ad-β-gal adenoviral vector (33.1±13.2 vs. 1.0±0.1, $p<0.01$, expressed in relative quantitation, n=3 for each group). In contrast, co-transfection with Ad-DN-c-Jun dramatically suppressed transcription of MMP-13 gene (1.8±0.2 in relative quantitation). Meanwhile, MMP-13 expression of Ad-Cyr61-transfected VSMCs was maintained in part after doxycycline treatment (6.0±3.1 in relative quantitation), but this score is much lower than that of VSMCs without doxycycline treatment ($p<0.01$). This depression of MMP-13 transcription is in line with the previous report. (23) Zinc-chelating tetracyclines such as doxycycline have an inhibitory effect on enzymatic activities of MMPs. As well as this chelating effect, tetracycline can also indirectly suppress protein expression of MMPs.

And because many MMP proteins are usually activated by other members of MMP proteins, so doxycycline also can inhibit their proteolytic enzyme activation. Suppressed MMP-13 expression of doxycycline-treated VSMCs might be connected to these properties of doxycycline.

Interestingly, MMP-9 transcription in VSMCs was not stimulated after CYR61 transfection (0.8±0.2 in Ad-Cyr61-transfected VSMCs vs. 1.0±0.1 in VSMCs with control Ad-β-gal adenoviral vector at the day 3 after the transfection, p=0.76). This result was in line with our microarray analysis. At the time of 24 hours after the transfection, MMP-9 gene transcription was not significantly enhanced by Ad-Cyr61 transfection (only 1.2-fold compared to control). Co-treatment with Ad-DN-c-Jun or doxycycline also did not make any notable differences.

Enzymatic activity of MMP-9 is augmented in CYR61-transfected VSMCs

Our results indicated that mRNA transcription and protein expression of all MMPs such as MMP-9 were not immediately increased in the process of CYR61-mediated ectopic calcification. But, some MMPs can be activated by other MMP proteins, and as an instance, MMP-9 is a well-known non-ECM substrate of MMP-13. (18) In this context, owing to the stimulated expression of MMP-13 in Ad-Cyr61-treated VSMCs, we hypothesized that enzymatic activity

of MMP-9 would be increased. To confirm this idea, gelatin zymography was repeatedly tested during 14 days after the transfection, and the result is shown in Figure 3-1. Serial examinations of zymography revealed that enzymatic activity of MMP-9, opposed to the absolute level of mRNA transcription, was constantly increased by CYR61-mediated expression of MMP-13.

Meanwhile, enzymatic activity of MMP-9 was suppressed in Ad-DN-c-Jun adenoviral vector or doxycycline-treated VSMCs. In contrast to the house-keeping pro-MMP-2 (18), at the time of 3 days after the transfection, MMP-9 activity was turned up only in Ad-Cyr61-treated VSMCs. (Figure 3-2) Active form of MMP-9 as well as pro-MMP-9 was clearly manifested only in Ad-Cyr61-treated VSMCs. Even though Ad-Cyr61 was also treated to VSMCs for Ad-Cyr61/Ad-DN-c-Jun co-transfection, MMP-9 activity did not come to the front in this case. Doxycycline treatment also suppressed enzymatic activity of MMP-9 as expected.

MMP-13-mediated MMP-9 activation was also demonstrated in blocking experiment using siRNA for MMP-13. Compared to the positive control, MMP-9 activation in Ad-Cyr61-transfected VSMCs was obviously suppressed by siRNA for MMP-13 (Figure 3-3). Both MMP-13 and MMP-9 are known to be independently activated by plasmin or other MMP family members such as MMP-2 (gelatinase), MMP-3 (stromelysin-1) and MMP-10 (stromelysin-2). (18, 19) However, our results indicated that activation of MMP-9 in mouse

VSMCs was caused mainly by MMP-13 expression.

CYR61 activation in VSMCs and vascular calcification are connected to the disruption of ECM via JNK/MMP pathway

MMP-9 activation by MMP-13 can be thought as some sort of signal amplification. In this regard, initiation or propagation of CYR61-mediated ectopic calcification might be influenced by this amplified molecular cascade, and altered ECM dynamics would contribute to calcification process. This hypothesis was tested and summarized in Figure 4 and 5. Using the electron microscopy, degraded ECM and digested adherent junctions between transfected VSMCs were confirmed at the time of post-transfection day 14 (Figure 4). During the incubation period, Ad-Cyr61-treated VSMCs were detached from the culture plate, and cell-to-cell connections broke down. Suppression of CYR61 expression with Ad-DN-c-Jun vector could prevent this disruption to some degree, and doxycycline treatment can attenuate CYR61-mediated ECM degradation almost entirely. In contrast, cell-to-cell adherent junctions of MMP-9 knockout VSMCs were not recovered by Ad-DN-c-Jun transfection or doxycycline treatment.

The same tendency was also confirmed by light microscopic examination. Von Kossa staining was used to differentiate the mineralization potency of cultured cells. Mineralization was prominent in Ad-Cyr61-treated wild type VSMCs (Figure 5). But, calcium

phosphate deposition was somewhat reduced by Ad-DN-c-Jun co-transfection, and mineralization was diminished one step further by doxycycline treatment.

Discussion

CYR61, one of matricellular proteins belongs to CCN gene family (CCN1), was originally cloned as an immediate early gene expressed in growth factor-stimulated fibroblasts. (26) This protein regulates various cellular processes such as cell adhesion, migration, proliferation, survival and apoptosis/senescence. And by modulating these aspects in a cell-specific manner, CYR61 proteins can coordinate complex cell-to-cell interaction and contribute to the processes of inflammation, wound healing and tissue repair. (14) Specifically in VSMCs, CYR61 directly regulates cell adhesion and chemotaxis via α6β1 integrin and heparan sulfate proteoglycan. (27)

In our experiments, activation of CYR61 was connected to the disorganized intercellular gap junctions around the Cyr61-transfected VSMCs. This change was mediated by elevated expressions of some MMPs such as MMP-13, MMP-3 and MMP-10. Interestingly, these MMPs commonly have an AP-1 binding site as a promoter in their genes. (18, 19) Our results confirmed that down-regulation of a component of AP-1 transcription factor, i.e., c-Jun with Ad-DN-c-Jun transfection, resulted in suppressed expression of MMP-13. Meanwhile, MMP-13 activation was linked to augmented enzymatic activity of MMP-9. Boosted activity of MMP-9 could be seen as some sort of CYR61-triggered signal amplification in VSMCs. In addition, local imbalance between MMPs and TIMPs provoked by CYR61 may augment activities of MMPs one step further and can

lead to pathologic ectopic mineralization. Molecular effects of CYR61 in VSMCs might be crystallized in this way, and these complex interactions among several key molecules regarding matrix degradation may be important in the initial phase of calcification process.

Indeed, our data suggest that vascular calcification was interrelated to the alterations in ECM dynamics. Ectopic mineralization of Ad-Cyr61-transfected VSMCs was markedly increased. This was coincided with ECM degradation and MMP-triggered break down of cell-to-cell adherent junctions. These results help us recognize some key molecules and their relations in the process of vascular calcification. In addition to our previous report on the connection of angiotensin Ⅱ, type 1 angiotensin receptor and CYR61, our data pointed that activated MMPs were identified as a downstream effector molecule in ectopic mineralization of VSMCs. In this context, doxycycline, a broad spectrum MMP inhibitor, was able to attenuate CYR61-mediated mineralization as well as ECM disruption in transfected VSMCs.

In fact, elastin degradation is important for the initiation and propagation of vascular calcification. (28) Insoluble elastin can be degraded by MMPs including MMP-9. (18) The exact mechanism how degraded elastin accelerates vascular calcification is not yet certain. However, degraded elastin as a nucleating factor might have increased affinity for calcium binding. (29) And therefore, ectopic

growth of hydroxyapatite crystal along the elastic lamellae can be facilitated. (30) Previous report also pointed that elastin degradation during the initial steps of arterial medial calcification was substantially increased. (31) Added to this, TGF-β as well as soluble elastin peptides might also be released during MMP-mediated elastinolysis. (32) TGF-β might directly enhance the expression of other osteogenic genes in VSMCs, and this can stimulate vascular medial layer calcification. (2, 28) Although we could not identify the exact causal relationship between the ECM disruption and ectopic mineralization with our data, MMP-mediated ECM break-down was clearly indispensable for ectopic mineralization.

Cellular changes in VSMCs and enzymatic degradation of ECM can also provide more extended perspectives in vascular calcification. In VSMCs, pro-inflammatory signals such as angiotensin II can induce CYR61 as well as pro-fibrotic connective tissue growth factor (CCN2) and TGF-β. (2) In fact, CYR61 is known as a fibrosis-limiting functional regulator in the wound healing process. (14) In contrast to CCN2 and TGF-β, CYR61 (CCN1) can induce cellular senescence of myofibroblasts in the wounded tissue. Sufficient accumulation of senescent myofibroblasts is an important prerequisite for normal wound healing response and this process is controlled mainly by CYR61. (27) Accumulated CYR61 in granulation tissue may acts as an antifibrotic molecular switch to trigger cellular senescence. Phenotypic transition of myofibroblasts may ensue, and these cells can acquire senescence-associated secretory phenotype. Expressions of

various procollagen genes or TIMPs may be subsequently decreased as shown in our microarray analysis. Instead, expression of MMPs from senescent cells can be increased and matrix remodeling can be done in this context. (14) Thus, activation of MMPs in transdifferentiated VSMCs of calcifying vessel wall could be understood as an adaptive change in the wound healing process. In this manner, matrix remodeling and wound repair in the milieu of systemic inflammation can provide favorable conditions for nanocrystal nucleation and crystal growth under the morbid circumstances such as chronic kidney disease-related hyperphosphatemia. (1)

Meanwhile, CYR61 may offer another important potential mechanism in regard to the promotion of vascular calcification. Component protein of transcription factor AP-1, i.e., phosphorylated c-Jun is an immediate product of activated c-Jun N-terminal kinase (JNK), and this is a key molecule for the transcription of MMPs such as MMP-13. CYR61-MMP cascade in VSMCs is conveyed by this JNK signaling pathway. JNK activation triggered by CYR61 may be mediated by the elevated level of intracellular reactive oxygen species (ROS). (14) By binding to cell surface integrins and heparan sulfate proteoglycans, CYR61 can activate small GTPase RAC1 and NADPH oxidase 1. This leads to substantial elevation of ROS in VSMCs. ROS can induce DNA damage, and more importantly, can activate JNKs directly. In addition, activated JNKs can cause proteasomal degradation of cellular FLICE-like inhibitory protein

(FLIP), and this change may induce caspase 8-mediated cellular apoptosis. (14) In calcifying tissue, apoptosis of VSMCs provides small apoptotic bodies. These can act as important nucleating agents for calcium phosphate nanocrystal deposition. (28) In this way, CYR61-induced JNK activation may offer VSMCs-derived apoptotic bodies, and can contribute to the initial phase of calcification process. (1)

Conclusion

CYR61 is an important mediator of ectopic mineralization of VSMCs. MMPs such as MMP-13 and MMP-9 were identified as downstream effector molecules in our experiments. ECM remodeling and calcium phosphate crystal deposition were integrated in the signal cascade regarding JNK-mediated MMP expression. In Cyr61-transfected VSMCs, enhanced expression and augmented enzymatic activities of MMPs were prominent. And these changes were relayed into disorganization of cell-to-cell adherent junctions and ectopic mineralization of VSMCs. Therapies targeting this signaling cascade and enzymes may attenuate vascular calcification and would have therapeutic potential.

References

1. Lanzer P, Boehm M, Sorribas V, Thiriet M, Janzen J, Zeller T, St Hilaire C, Shanahan C. Medial vascular calcification revisited: review and perspectives. Eur Heart J 2014; 35: 1515-25.

2. Wu M, Rementer C, Giachelli CM. Vascular calcification: an update on mechanisms and challenges in treatment. Calcif Tissue Int 2013; 93: 365-73.

3. Shanahan CM. Inflammation ushers in calcification: a cycle of damage and protection? Circulation 2007; 116: 2782-5.

4. Bostrom K, Watson KE, Horn S, Wortham C, Herman IM, Demer LL. Bone morphogenetic protein expression in human atherosclerotic lesions. J Clin Invest 1993; 91: 1800-9.

5. Nguyen AT, Gomez D, Bell RD, Campbell JH, Clowes AW, Gabbiani G, Giachelli CM, Parmacek MS, Raines EW, Rusch NJ, Speer MY, Sturek M, Thyberg J, Towler DA, Weiser-Evans MC, Yan C, Miano JM, Owens GK. Smooth muscle cell plasticity: fact or fiction? Circ Res 2013; 112: 17-22.

6. Tang Z, Wang A, Yuan F, Yan Z, Liu B, Chu JS, Helms JA, Li S. Differentiation of multipotent vascular stem cells contributes to vascular diseases. Nat Commun 2012; 3: 875.

7. Shroff RC, McNair R, Skepper JN, Figg N, Schurgers LJ,

Deanfield J, Rees L, Shanahan CM. Chronic mineral dysregulation promotes vascular smooth muscle cell adaptation and extracellular matrix calcification. J Am Soc Nephrol 2010; 21: 103-12.

8. Schoppet M, Kavurma MM, Hofbauer LC, Shanahan CM. Crystallizing nanoparticles derived from vascular smooth muscle cells contain the calcification inhibitor osteoprotegerin. Biochem Biophys Res Commun 2011; 407: 103-7.

9. Diane Proudfoot JNS, Laszlo Hegyi, Martin R. Bennett, Catherine M. Shanahan, Peter L. Weissberg. Apoptosis regulates human vascular calcification in vitro: Evidence for initiation of vascular calcification by apoptotic bodies. Circ Res 2000; 87: 1055-62.

10. Aikawa E, Nahrendorf M, Figueiredo JL, Swirski FK, Shtatland T, Kohler RH, Jaffer FA, Aikawa M, Weissleder R. Osteogenesis associates with inflammation in early-stage atherosclerosis evaluated by molecular imaging in vivo. Circulation 2007; 116: 2841-50.

11. Jaffe IZ, Tintut Y, Newfell BG, Demer LL, Mendelsohn ME. Mineralocorticoid receptor activation promotes vascular cell calcification. Arterioscler Thromb Vasc Biol 2007; 27: 799-805.

12. Armstrong ZB, Boughner DR, Drangova M, Rogers KA. Angiotensin II type 1 receptor blocker inhibits arterial

calcification in a pre-clinical model. Cardiovasc Res 2011; 90: 165-70.

13. Na S-H. Angiotensin II promotes vascular smooth muscle cell calcification via cysteine-rich protein 61 activation. Doctoral thesis, Seoul National University 2009.

14. Jun JI, Lau LF. Taking aim at the extracellular matrix: CCN proteins as emerging therapeutic targets. Nat Rev Drug Discov 2011; 10: 945-63.

15. Yu Y, Gao Y, Wang H, Huang L, Qin J, Guo R, Song M, Yu S, Chen J, Cui B, Gao P. The matrix protein CCN1 (CYR61) promotes proliferation, migration and tube formation of endothelial progenitor cells. Exp Cell Res 2008; 314: 3198-208.

16. Zhou D, Herrick DJ, Rosenbloom J, Chaqour B. Cyr61 mediates the expression of VEGF, alphav-integrin, and alpha-actin genes through cytoskeletally based mechanotransduction mechanisms in bladder smooth muscle cells. J Appl Physiol (1985) 2005; 98: 2344-54.

17. Kim H-S, Carsten S, Henrike M, Ichiro S, Yuri I, Yoon S-W, Park Y-B, Kenneth W. Akt/FOXO3a signaling modulates the endothelial stress response through regulation of heat shock protein 70 expression. FASEB J. 2005;19:1042-1044.

18. Sajal Chakraborti MM, Sudip D, Amritlal M, Tapati C. Regulation of matrix metalloproteinases: an overview. Mol Cell

Biochem. 2003;253:269-285.

19. Fanjul-Fernandez M, Folgueras AR, Cabrera S, Lopez-Otin C. Matrix metalloproteinases: evolution, gene regulation and functional analysis in mouse models. Biochim Biophys Acta 2010; 1803: 3-19.

20. Yasumoto H KS, Zhan Y, Miyazaki H, Hoshiga M, Kaneda Y, Morishita R, Iwao H. Dominant negative c-Jun gene transfer inhibits vascular smooth muscle cell proliferation and neointimal hyperplasia in rats. Gene Therapy 2001; 8: 1682-9.

21. Sanae Miyake MM, Yumi Kanegae, Shizuko Harada, Yumi Sato, Koichi Takamori, Chikashi Tokuda, Izumu Saito. Efficient generation of recombinant adenoviruses using adenovirus DNA-terminal protein complex and a cosmid bearing the full-length virus genome. Proc Natl Acad Sci USA 1996; 93: 1320-4.

22. Aesim Cho JG, Michael A. Reidy. Mitogen-activated protein kinases mediate matrix metalloproteinase-9 expression in vascular smooth muscle cells. Arterioscler Thromb Vasc Biol 2000; 20: 2527-32.

23. Zakeri B, Wright GD. Chemical biology of tetracycline antibiotics. Biochem Cell Biol 2008; 86: 124-36.

24. Johnson JL, Dwivedi A, Somerville M, George SJ, Newby AC. Matrix metalloproteinase (MMP)-3 activates MMP-9 mediated

vascular smooth muscle cell migration and neointima formation in mice. Arterioscler Thromb Vasc Biol 2011; 31: e35-44.

25. Montezano AC, Zimmerman D, Yusuf H, Burger D, Chignalia AZ, Wadhera V, van Leeuwen FN, Touyz RM. Vascular smooth muscle cell differentiation to an osteogenic phenotype involves TRPM7 modulation by magnesium. Hypertension 2010; 56: 453-62.

26. Timothy P. O'brien, George P. Yang, Laura Sanders, Lau LF. Expression of cyr61, a growth factor-inducible immediate-early gene. Molecular and cellular biology 1990; 10: 3569-77.

27. Chen CC, Lau LF. Functions and mechanisms of action of CCN matricellular proteins. Int J Biochem Cell Biol 2009; 41: 771-83.

28. Pai AS, Giachelli CM. Matrix remodeling in vascular calcification associated with chronic kidney disease. J Am Soc Nephrol 2010; 21: 1637-40.

29. Spina M FA, Ewins AR, Parker KH, Winlove CP. Physicochemical properties of arterial elastin and its associated glycoproteins. Biopolymers 1999; 49: 255-65.

30. Basalyga DM, Simionescu DT, Xiong W, Baxter BT, Starcher BC, Vyavahare NR. Elastin degradation and calcification in an abdominal aorta injury model: role of matrix metalloproteinases. Circulation 2004; 110: 3480-7.

31. Janzen J VP. Arterial calcifications: morphological aspects and their pathological implications. Z Kardiol 2001; 90: 6-11.

32. Watson KE, Bostrom K, Ravindranath R, Lam T, Norton B, Demer LL. TGF-beta 1 and 25-hydroxycholesterol stimulate osteoblast-like vascular cells to calcify. J Clin Invest 1994; 93: 2106-13.

Table 1. Primers used to amplify mRNAs encoding mouse Cyr61, MMP-9/MMP-13, Runx2, GAPDH

Genes	Accession number	Primer		Product size (bp)	Cycle number	Annealing temperature (°C)
Cyr61	NM_010516	Sense	5'-cagttagatgtcagtgcg-3'	283	33	60
		Antisense	5'-aagtcctctgtcattccc-3'			
MMP-9	NM_004994	Sense	5'-acctcgaactttgacagcgac-3'	133	35	62
		Antisense	5'-gaggaatgatctaagcccagc-3'			
MMP-13	NM_002427	Sense	5'-atgactgaggctccgaga-3'	113	35	65
		Antisense	5'-acctaaggagtggccgaact-3'			
Runx2	NM_001146	Sense	5'-aattgcaggcttcgtggttg-'3	136	38	60
		Antisense	5'-tcccctgaatggctgtatggt-3'			
GAPDH	M32599	Sense	5'-accacagtccatgccatcac-3'	450	15	65
		Antisense	5'-caccaccctgttgctgtagcc-3'			

Table 2. Summary of activated and suppressed molecules with adenoviral transfection of Ad-Cyr61

Reporter name	Time lapse after the transfection with Ad-Cyr61	
	4 hours (fold)	24 hours (fold)
Matrix metalloproteinase 13 (MMP-13)	55.33	7.89
Matrix metalloproteinase 3 (MMP-3)	49.87	6.54
Matrix metalloproteinase 10 (MMP-10)	6.41	2.03
Matrix metalloproteinase 8 (MMP-8)	5.24	2.01
Tissue inhibitor of metalloproteinase 3 (Timp3)	0.76	0.72
Tissue inhibitor of metalloproteinase 2 (Timp2)	0.43	0.62
Procollagen, type IV, alpha 5	0.72	0.95
Procollagen N-endopeptidase, type III	0.69	0.74
Procollagen C-endopeptidase enhancer protein	0.68	0.82
Procollagen, type II, alpha 1	0.62	0.65
Procollagen, type V, alpha 2	0.55	0.80
Procollagen, type X, alpha 1	0.55	0.60
Procollagen, type XVI, alpha 1	0.54	0.71
Procollagen, type XVIII, alpha 1	0.50	0.73
Procollagen, type IV, alpha 1	0.44	0.59
Procollagen, type VI, alpha 2	0.40	0.71
Procollagen, type V, alpha 1	0.35	0.53
Procollagen, type XXVIII, alpha 1	0.32	0.64

Figure 1. CYR61-mediated JNK/MMP activation in cultured VSMCs

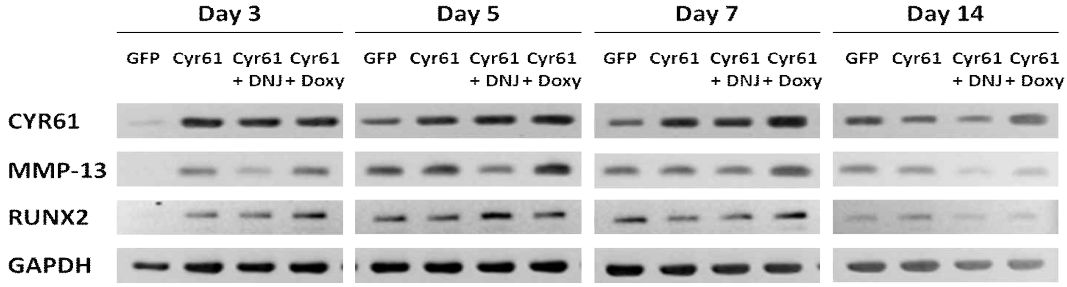

Abbreviations: GFP; green fluorescence protein, Cyr61; cysteine-rich angiogenic protein 61, DNJ; dominant-negative mutant of c-Jun, Doxy; doxycycline, MMP-13; matrix metalloproteinase 13, RUNX2; runt-related transcription factor 2,

Wild type mouse VSMCs were transfected with 50 MOIs of GFP-containing control adenoviral vector or Ad-Cyr61 vector. And two sets of Ad-Cyr61-treated VSMCs were co-treated with Ad-DN-c-Jun adenoviral vector or 10μM/L of doxycycline. These 4 cell groups were incubated in calcification media containing 0.1μmol/L angiotensin Ⅱ, and harvested at the time of day 3, 5, 7, and 14. Protein expression profiles of CYR61, MMP-13, RUNX2 and GAPDH were systematically examined with immunoblot analysis using their corresponding primary antibodies. MMP-13 expression was suppressed by Ad-DN-c-Jun co-transfection, but doxycycline (broad-spectrum MMP inhibitor) treatment was not conveyed to significant reduction in MMP-13 expression. Osteoblastic transdifferentiation by Ad-Cyr61 transfection was confirmed with immunoblotting for RUNX2. RUNX2 expressions were not influenced by Ad-DN-c-Jun or doxycycline administration.

Abbreviations: GFP; green fluorescence protein, Cyr61; cysteine-rich angiogenic protein 61, DNJ; dominant-negative mutant of c-Jun,

Doxy; doxycycline, MMP-13; matrix metalloproteinase 13, RUNX2; runt-related transcription factor 2, GAPDH; glyceraldehyde 3-phosphate dehydrogenase

cf. Cyr61 + DNJ means co-transfection of Ad-Cyr61 and Ad-DN-c-Jun, and Cyr61 + Doxy means 10μM/L doxycycline treatment for Ad-Cyr61-transfected VSMCs.

Figure 2. Transcription of MMP-13, but not for MMP-9, was increased by CYR61

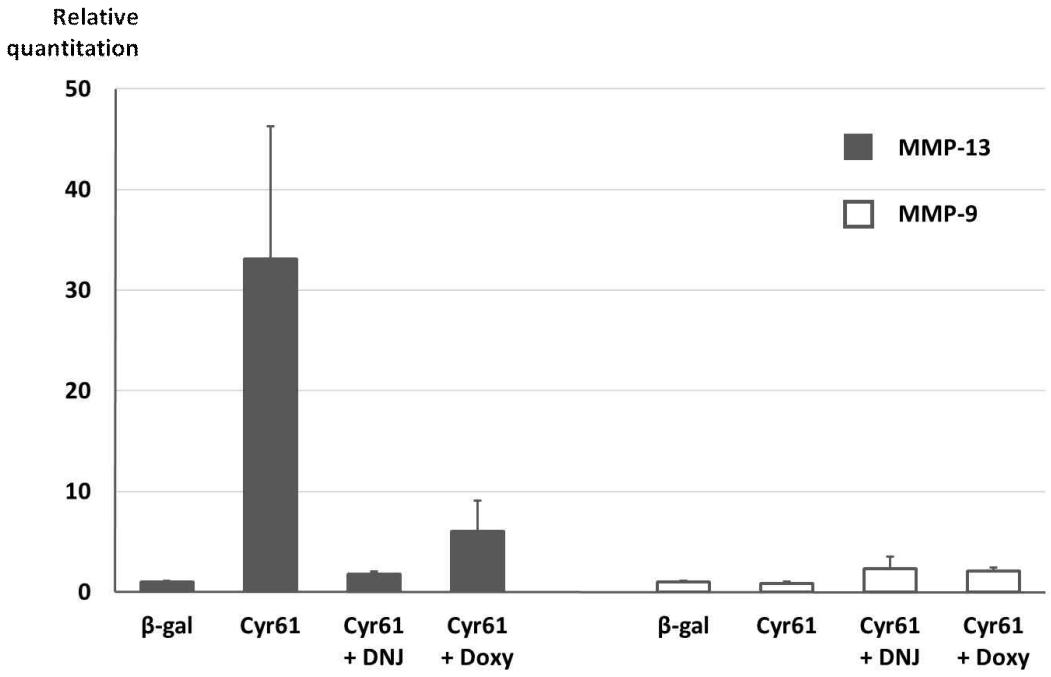

Expression of MMP-13 was amplified only in Cyr61-transfected VSMCs. Treatment of adenoviral vector containing dominant negative mutant of c-Jun or doxycycline suppressed the transcription level of MMP-13. In contrast to MMP-13, MMP-9 transcription was not stimulated after CYR61 transfection.

Abbreviations: β-gal; adenoviral vector containing bacterial β-galactosidase gene (Ad- β-gal), DNJ; adenoviral vector containing dominant-negative mutant of c-Jun, Doxy; doxycycline

Figure 3. Activated MMP-9 in Ad-Cyr61-transfected VSMCs and blocking experiments for c-Jun/MMP

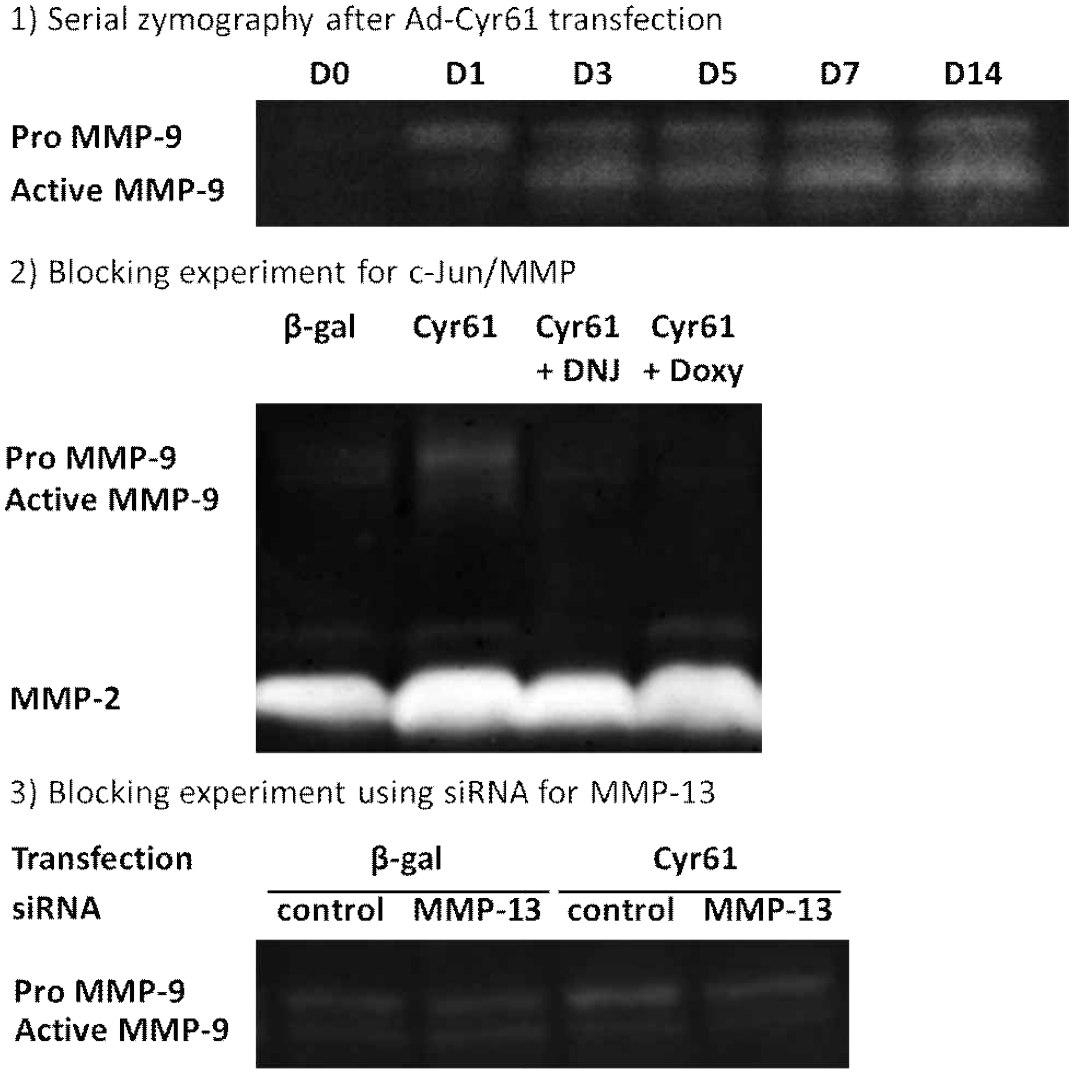

1 and 2) In Ad-Cyr61-transfected VSMCs, transcription level of MMP-9 was not increased, but enzymatic activity of MMP-9 was markedly augmented. Enhanced MMP-9 activity was prominent only in Ad-Cyr61-transfected VSMCs. MMP-9 activity was diminished almost entirely by the treatment of adenoviral vector containing

dominant negative mutant of c-Jun or doxycycline.

3) Blocking experiment with siRNA for MMP-13 confirmed that MMP-9 was activated by MMP-13 in Ad-Cyr61-transfected VSMCs. siRNA for MMP-13 successfully reduced the amount of active form MMP-9.

Figure 4. Degraded extracellular matrix and digested adherent junctions by MMPs via CYR61 activation in mouse VSMCs

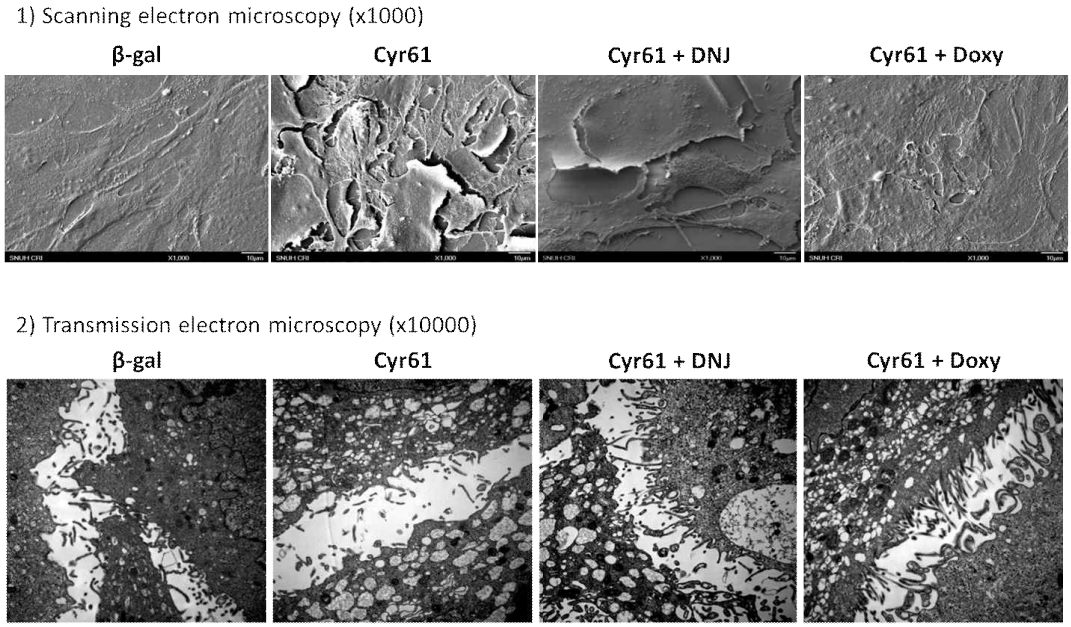

1) The electron microscopic examinations clearly confirmed that Cyr61-transfected VSMCs had disrupted extracellular matrices (ECMs) around the cells. However, when MMP activities were suppressed with Ad-DN-c-Jun co-transfection or doxycycline treatment, Cyr61-mediated ECM disruption could be markedly attenuated or almost entirely diminished.

2) Cell-to-cell adherent gap junctions and microfilaments on the surface of VSMCs were disorganized with the transfection experiment using the Ad-Cyr61 vector. Again, this effect of CYR61 was successfully minimized with Ad-DN-c-Jun co-transfection or doxycycline treatment. These changes were in accordance with the findings of scanning electron microscopy.

Figure 5. Von Kossa staining for VSMCs mineralization according to various conditions

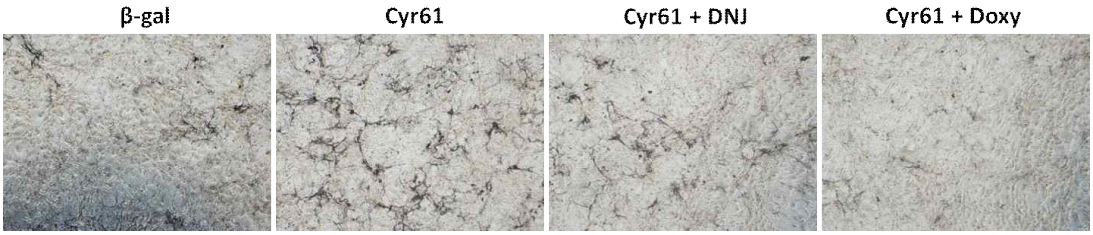

Ectopic mineralization was significantly enhanced by CYR61 in transfected VSMCs. As shown in this examination, the extent and severity of mineralization were decreased by Ad-DN-c-Jun co-transfection or doxycycline treatment. Interestingly, these changes in mineralization were coincided with the changes of ECM disruption according to the respective conditions.

한글 초록

김치훈

분자의학 및 바이오제약학과

융합과학기술대학원, 서울대학교

배경: Cysteine-rich angiogenic protein 61(CYR61)은 혈관 평활근 세포에서 안지오텐신 II를 유도하며, 골형성 교차분화를 일으킨 혈관 평활근 세포에서 이소성 무기화(석회화)를 조절하는 주요 조절인자이다. CYR61에 의해 유도된 무기화의 정확한 분자 기전에 대해서는 보고가 많지 않아 본 연구자는 CYR61에 의해 매개되는 분자 효과의 하위 구조를 규명해보고자 하였다.

연구 방법 및 결과: C57BL6 생쥐의 흉부 대동맥에서 얻은 혈관 평활근 세포를 배양한 다음, Cyr61을 포함한 아데노바이러스 벡터를 이용하여 세포를 감염시킨 후 CYR61이 혈관 평활근 세포의 무기질화에 미치는 영향을 평가하기 위해 마이크로어레이 실험을 진행하였다. 세포 감염 실험 시행으로부터 24시간 후 MMP-13, MMP-3, MMP-10과 같은 몇 가지 기질금속단백분해효소가 각각 7.9배, 6.5배, 2.0배로 즉각적으로 그 발현이 증가하였다. 하지만 TIMP-3와 TIMP-2와 같은 기질금속단백분해효소의 억제 인자들은 각각 52%와 71%가 감소하였다. ($p<0.05$) 실시간 중합효소연쇄반응 실험으로 대조군 바이러스 벡터에 감염시킨 혈관 평활근 세포에 비해 Cyr61 포함 아데노바이러스 벡터에 감염시킨 혈관 평활근에서 MMP-13의 발현이 33±13배 증가한다는 점도 확인하였다 ($p<0.05$). 이와 달리 MMP-9의 mRNA 발현은 증가하지 않았는데, 그 대신 효소 활성 분석 방법을 통해 MMP-9의 효소 활성이 Cyr61 포함 아데노바이러스 벡터 감염 혈관 평활근 세포에서 증가함

을 밝혔다. 한편, MMP-13의 짧은 간섭 RNA를 추가 처리한 혈관 평활근 세포에서는 MMP-9의 활성이 다시 큰 폭으로 감소하였다. Von Kossa 염색법을 이용한 현미경 관찰이나 전자 현미경 검사 소견에서는 c-Jun 단백에 대한 우성음성돌연변이체를 포함한 아데노바이러스 벡터를 처리하거나, 아니면 여러 기질금속단백분해효소의 억제제의 기능을 가진 독시사이클린을 처리하는 경우, CYR61에 의해 매개되는 세포 외 기질의 파괴 및 이소성 무기질화가 최소화되거나 상대적으로 완화됨을 확인하였다.

결론: 이런 소견들은 CYR61에 의해 매개되는 기질금속단백분해효소의 활성화가 염증 유발 환경 하에서 혈관 석회화를 유발하는 데 있어 중요한 기전으로 작동한다는 점을 가리키는 근거가 될 수 있다. CYR61이나 기질금속단백분해효소를 조절할 수 있는 치료법이 개발된다면 혈관 석회화를 조절할 수 있게 될 것이고, 임상 현장에서도 유용하게 쓰일 수 있을 것이다.

Key words: Cysteine-rich angiogenic protein 61, Matrix metalloproteinase, Mineralization, Vascular calcification

Student Identification Number: 2010-22901